Antarct. Meteorite Res., **11**, 136–154, 1998

SAMPLE PROCESSING AND INITIAL ANALYSIS TECHNIQUES FOR ANTARCTIC MICROMETEORITES

Hajime YANO[1] and Takaaki NOGUCHI[2]

[1]*Planetary Science Division, Institute of Space and Astronautical Science, Yoshinodai 3-chome, Sagamihara 229-8510*
[2]*Department of Materials and Biological Sciences, Ibaraki University, Bunkyo 2-chome, Mito 310-0056*

Abstract: Based on our initial visual selection (IVS) criteria and low vacuum (LV)-SEM/EDS data, we successfully selected candidates of unmelted chondritic Antarctic micrometeorites (AMMs) from the unsorted sample set collected by Maurette's group in 1991. AEM data of some of the selected microparticles show that they are unmelted but probably dehydrated AMMs. An AMM candidate, 91-1-C4, contains ferroan (around Fo30) olivine grains which have planar channels parallel to (001). Their textures quite resemble those shown in the initial stage of iddingsite formation of olivine phenocrysts in terrestrial basalts. These findings indicate that some olivine crystals in AMMs can be altered even in the Antarctic environment.

1. Introduction

Micrometeoroids in size range of ~50–500 μm are considered to be a major contributor for the mass accretion of extraterrestrial material on the Earth of $4\pm2\times10^{10}$ g per year (LOVE and BROWNLEE, 1993), whereas stratospheric interplanetary dust particles (IDPs) (*i.e.* 1 μm <diameter (d) <50 μm) and conventional meteorites (<10^{10} g) generally make up only 1% of the total mass (GRÜN *et al.*, 1985). Blue lakes in Greenland and ice sheets in Antarctica provide high concentrations of micrometeorites (MAURETTE *et al.*, 1987, 1991). In addition, Antarctica is the most remote land from major industrial nations and continental winds keep the surface snow dry and relatively clean. Unlike the micrometeorites from Greenland blue lakes, Antarctic micrometeorites (AMM) are preserved in "cryconite-free" blue ice sheets and provide complementary insights of extraterrestrial materials collected from other terrestrial environments (*i.e.* stratosphere and deep sea sediments) and Low Earth Orbit (LEO).

Since 1994, one of the authors (HY) has been trained in the initial selection and processing of melted and unmelted AMMs with M. Maurette's group in the CSNSM, Orsay, France, mainly for comparative studies with micrometeoroid impacts in space (YANO, 1995; YANO *et al.*, 1996). In parallel to this effort, the Japanese Antarctic Research Expedition (JARE) team is currently preparing for their first collection of AMMs near the Syowa Station and Yamato and Belgica Mountains in the 1997–1999 term (KOJIMA, 1997). Thus it is our intention to establish a curation system for AMMs which is consistent with previous work outside Japan.

While some detailed studies of samples from the same collection with EPMA (YADA

et al., 1997), this paper focuses on standardizing selection criteria of AMMs from mixtures with terrestrial and artificial particles and sample processing for initial characterization of the microparticles using low vacuum SEM/EDS (LV-SEM/EDS) and TEM, including the ultra-microtoming technique.

2. Sample Collection in Antarctica

Since 1983, extraction of AMMs from deep ice cores (depth ~100–700 m) has been attempted by the Japanese Antarctica expedition team, as a by-product of a paleo-climatic survey near Mizuho Station, Asuka Station and the Advance Camp (HIGASHI and FUJII, 1994; YANO, 1991). Yet the small volumes of ice cores used for this effort were much less efficient to collect AMMs than filtering melt water of shallow ice. In 1988, a "micrometeorite factory" was constructed near the French station at Cap-Prudhomme (MAURETTE *et al.*, 1991). Steam generators were used to deliver water jets at 70–80 °C into a 2–3 m deep drilled hole and made a melt ice pocket in the blue ice sheet. The stream of melt water was filtered with four stainless steel sieves of 25, 50, 100 and 400 μm size holes to separate the microparticles by these size fractions. In December 1990 to January 1991, they melted 260 t more of blue ice. They repeated the AMM excavation with an improved micrometeorite factory (*i.e.* cleaner from in-house contamination) at Cap-Prudhomme in December 1993 to February 1994. Excluding the most recent samples, MAURETTE *et al.* have extracted ~40000 AMMs from 360 t of blue ice in total (MAURETTE *et al.*, 1994).

The samples analyzed in this study were collected at a blue ice field near Cap-Prudhomme, Antarctica in January 1991 by Maurettes' team. One bottle of "unprocessed" samples of 50–100 μm-sized particles sieved from 1 t of ice melt water, out of 100 t ice in total, was allocated to us. As can be seen from past reports, one of the key issues in the timely and systematic curation of abundant AMMs (*e.g.* in order of 10^3–10^4 samples per campaign) is how quickly and precisely one can distinguish AMMs from terrestrial and artificial microparticles. The first step of this challenge is a reduction of terrestrial and artificial inclusions in sieved samples. This requires a careful choice of collection sites in terms of contamination level (*i.e.* remoteness from exposed lands and human bases) and thorough design and operation of the "micrometeorite factory", or a ice melting and sieving instrument, on selection sites. After that, simple but reliable selection criteria of AMMs with only optical properties, morphology and X-ray EDS spectra must be established (*e.g.* CDPET (1981–1994) for stratospheric IDPs and ZOLENSKY *et al.* (1993) for impact craters on Low Earth Orbit spacecraft).

3. Experimental Procedure

(1) Initial visual selection (IVS) with a brush under a stereo optical microscope was performed at ISAS, Kanagawa, Japan. Among some thousands of the unsorted microparticles in the processed bottle, 50 AMM candidates were selected and placed onto a brass sample holder (6×6 matrix).

(2) The AMM candidates were observed by a low vacuum (LV-) SEM equipped

with EDS (JEOL JSM-5300LV and Oxford Link ISIS EDS system) at the Venture Business Laboratory, Tokyo Institute of Technology (TiTech), Tokyo, Japan. During the SEM/EDS observation and analysis, 20 terrestrial contaminants were identified by the combination of backscattered electron photomicrographs and EDS spectra.

(3) AMM candidates were embedded in a low-viscosity epoxy resin, TAAB Spurr kit. Ultramicrotomy was performed at the Center for Instrumental Analysis, Ibaraki University, Ibaraki, Japan using a Reichert-Leica Super Nova. Thickness of untramicrotomed sections was ~100 nm.

(4) The sections were observed by AEM (JEOL JEM-2000 FX II TEM equipped with Philips DX4 energy dispersive X-ray analysis system) at the Center for Instrumental Analysis, Ibaraki University. Quantitative analysis was based on the Cliff-Lorimer thin film approximation. Experimental k factors were determined from many mineral standards.

4. Initial Processing

Among the above, a key for time-saving and reliable curation is to establish a routine training program of "initial visual selection" (IVS) of AMM candidates from obvious terrestrial and artificial contamination before carrying out further analyses. Here we adapted the criteria with the stratospheric IDPs by CDPET (Table 1) and inherited Maurette's technique for the selection to prevent or minimize loss and post-capture contamination of the samples.

However, it should be noted that this preliminary criteria is valid mainly for chondritic AMMs. This is by no means a tool for the final judgment of finding all types of extraterrestrial particles, such as non-chondritic ones, for instance Ca- and Al-rich inclusion-like micrometeorites. Also glassy melted AMMs were found in the past (*e.g.* YANO, 1995). We admit that there are always a group of particles of non-trivial origins between the "possible chondritic AMMs" group and the "obvious terrestrial contamination" group. We must not discard such particles before applying detailed analyses to them. However, such a group held only a few% of the total in this study and it has been kept for future studies.

First of all the sample bottle was washed with distilled water and deposited all the grains on to a paper filter under an optical stereo-microscope. A new, fine water paint brush being wet with the distilled water was used as a "manipulator" to hold and move

Table 1. IVS criteria and typical EDX peaks for AMMs (Refer the CDC for stratospheric IDPs and LDEF results; CDPET, 1981–94 and ZOLENSKY et al., 1993).

	Possible AMM	Obvious contaminations
Morphology	spherical to porous	sheets, crystals
Color	black to brown	red, yellow, white
Transparency	opaque	translucent, transparent
Luster	dull	metallic
EDX peaks	Si≥Mg>Fe (olivine and pyroxene) with Al, S, Ca plus traces of Mn and/or Cr	—

several hundreds of the microparticles to separate possible AMM candidates from obvious contamination. The following contaminants were identified and separated from the AMM candidates:

(1) terrestrial morainic debris such as silicate grains from surrounding mountains,
(2) fragments of penguin and other bird feathers (!),
(3) ashes ejected from the chimney of the steam generator engine,
(4) fragments released from plastic tubes, and
(5) rust from corrosion of steam generator pipes and the pumps made of ordinary steel.

The first group included such as crystal quartz, feldspar, mica, ilmenite suggesting continental and volcanic origin (YANO, 1991). In particular platelet grains were abundant in this size range compared to larger size regimes (*e.g.* 100–400 μm). Presence of bird feathers indicates that the collection site is near the coast close enough to receive other oceanic materials. In fact, oceanic materials like sea salt crystals and biological materials were found from surface snows collected by the 30th Japanese Antarctic Research Expedition (JARE-30) team around the Japanese Advance Camp (74°12'S, 34°59'E), where was even about 500 km away from the closest coast line at >3000 m elevation, much more inland than the Cap Prudhomme station (YANO, 1991; HIGASHI *et al.*, 1992). YANO (1991) subdivided 174 microparticles from the Asuka Station and Nansen ice field of Antarctica into their origins by referring to obtained data such as morphology, size, reflection, elemental composition and estimated age and location they accumulated. The classification of origin included (1) artificial vs. natural, (2) terrestrial *vs.* extraterrestrial, (3) continental (*e.g.* moraine debris), volcanic (*e.g.* sea salt, globular particles) and biological among the terrestrial particles, and (4) pollen, spore, plant opal, diatom, microfossils, etc. among the biological particles (Fig. 1). Examples of SEM

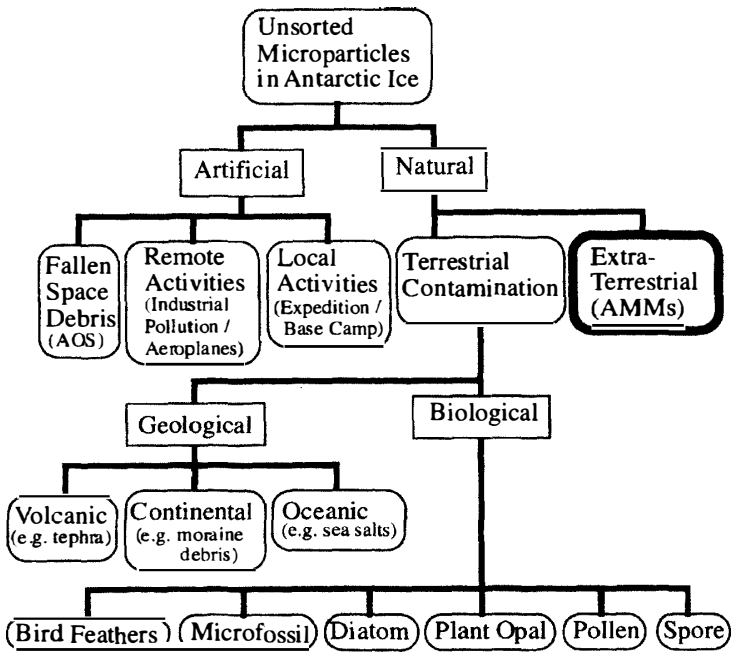

Fig. 1. Subdivisions of microparticles collected from ice cores and surface snow in Antarctica (modified from YANO, 1991).

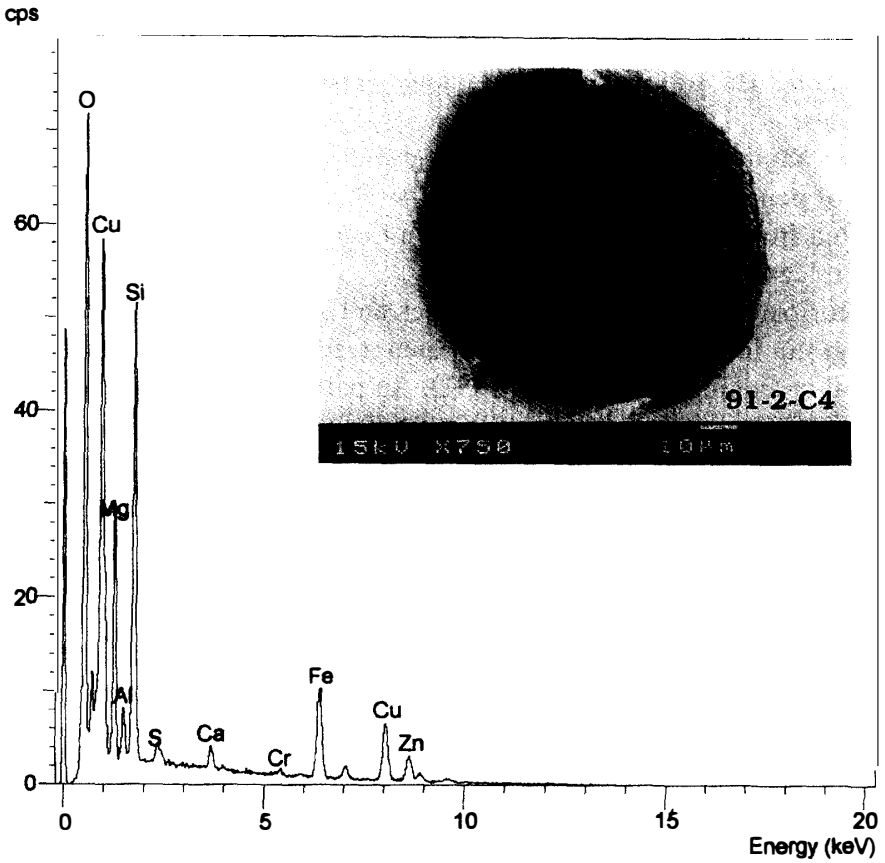

Fig. 2. EDS spectrum for sample 91-2-C4, a cosmic spherule. Inset: its BEI photograph. Many light-gray spots (fine-grained magnetite) exist on the surface of this sample. Fine-grained magnetite crystals are concentrated in upper left of the sample. This spectrum has major peaks of Si>Mg>Fe>Al>Ca = S >> Cr in the order of height. Sample size is ~88×80 μm.

images and EDS spectra of such terrestrial contamination can also be referred elsewhere (*e.g.* NISHIO *et al.*, 1985; SASE *et al.*, 1988; KUMAI and LANGWAY, 1990; HIGASHI *et al.*, 1990; HIGASHI and FUJII, 1994).

Another contaminant frequently found was reddish colored rust grains as reported in the last group. The 1991 collection suffered from such a contamination with rust particles, because the tubing of three steam generators used to melt ice were made of ordinary steel. To eliminate these, we carefully turned over even black colored grains with the wet brush and removed them if showing even the thinnest speck of red colored surfaces. However this operation still leaves some ambiguity for selection because most of partially melted (scoriaceous) AMMs have magnetite that can be oxidized during the interaction with ice water. Similarly terrestrial iron particles also rust in red first (iron hydroxide), but become dark (magnetite type) after further oxidation. Because fine-grained terrestrial volcanic glass beads are also present, all the black particles with sub-μm to μm size magnetite rims may not be extraterrestrial. However, most of the volcanic glass beads can be excluded from "cosmic spherules", on the basis of their EDS spectra ("cosmic spherule": 91-2-C4; Fig. 2). We mounted black or glassy (olivine-like green-to-yellow color), irregular-shaped AMM candidates on a multiple (6×6 matrix) sample holder made of brass for the low vacuum (LV)-SEM/EDS studies.

5. LV-SEM/EDS Analysis

A total of 44 AMM candidates with 5 cosmic spherules were investigated by LV-SEM/EDS (JEOL JSM-5310LV) equipped with an Oxford-Link ISIS EDS system. The advantage of using LV-SEM/EDS from ordinary (high-vacuum) SEM is that samples do not require any conductive coating; thus they will not be contaminated during initial qualitative determination of bulk elements for curation/cataloguing.

Another method to observe samples without conductive coating is low voltage (a few kV) scanning electron microscopy. The spatial resolution of backscattered electron images (BEIs) is lower than that of secondary electron images (SEIs). Because only BEIs can be acquired by LV-SEM, the spatial resolution of the images acquired by LV-SEM is lower than that of secondary electron images taken at low accelerating voltage. It is also well known that SEM observation at low accelerating voltage permits investigation of the fine-structures of the surface of IDPs (*e.g.* figure in p. 50, in Analysis of Interplanetary Dust (1994), ed. by M.E. ZOLENSKY *et al.*). However, heavy elements in the sample will not be excited efficiently by such low energy electron beams. Therefore, scanning electron microscopy at low accelerating voltage is inadequate for collection of elemental abundances of the samples even qualitatively. On the contrary, LV-SEM/EDS

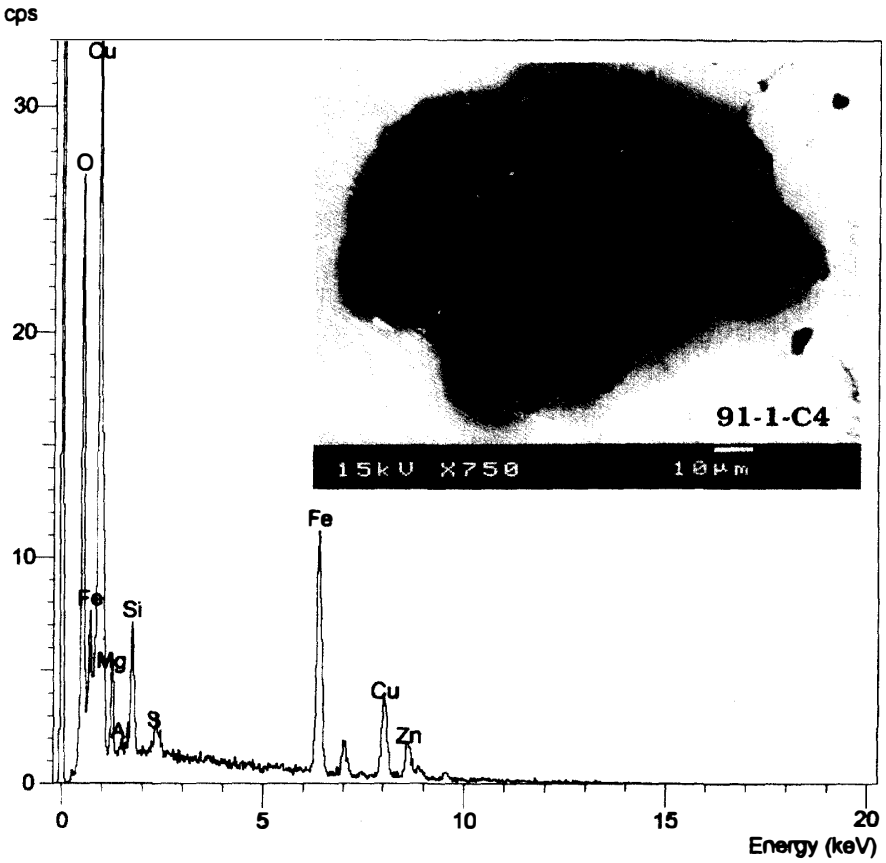

Fig. 3. EDS spectrum for sample 91-1-C4, an unmelted AMM candidate. Inset: its BEI photograph. This sample is irregular in shape. The BEI photograph shows that many light-gray globules (fine-grained magnetite crystals) cover the surface of this sample. This spectrum has major peaks of Si>Fe>Mg>S>Al in the order of height. Zn and Cu peaks are due to the brass holder. Sample size is ~110×76 μm.

can take as high accelerating voltage as 15 kV. Therefore, elements therein are excited well enough to give EDS spectra. 100 s live time was given for the EDS spectra. We could further identify terrestrial particles with multi-layer structure or melted droplets or clusters of large crystals. The remaining particles appeared porous and were usually covered with magnetite rims in sub-μm size.

EDS spectra of the unmelted AMM candidates (porous particles) typically had Si as the strongest peak followed by Mg or Fe, suggesting the existence of ferromagnesian silicates such as olivine, pyroxene, and some kind of clays. Figure 3 shows an EDS spectrum for such an unmelted AMM candidate, the sample 91-1-C4. It has major peaks of Si>Fe>Mg>>S>Al, in order of peak height. Relatively stronger peaks of Al, S and Ca were often apparent in cosmic spherules. In some cases, Cr and Ni peaks were also identified. A typical EDS spectrum of cosmic spherules (the sample 91-2-C4) shows major peaks of Si>Mg>Fe>Al>Ca=S>>Cr in the order of peak heights (Fig. 2). On the contrary, many terrestrial particles we found in this study include a large Fe peak with a small S peak while the others lacked Mg, but were enriched in Al and light elements like K and Cl.

6. Ultra-Microtoming and TEM Analysis

By combining the micro-morphology and qualitative EDS results, it appeared straightforward to identify unmelted or least-melted AMM candidates. The samples were ultra-microtomed for TEM analysis.

After being embedded in epoxy resin and sliced by an ultramicrotome, two of the least-melted AMM candidates with likely extraterrestrial EDS features were observed with TEM. One of them was a sample "guaranteed" as an AMM by Maurette's group (94-22-5) through their selection criteria. Another particle (91-1-C4) was selected by the procedure described above.

6.1. Mineralogy of the AMM candidates

Figure 4 is a low-magnification bright-field image of particle 94-22-5. Grain sizes of the constituent minerals vary from <50 to about 300 nm across. Dark-field image of the particle displays that it is composed mainly of fine-grained olivine and low-Ca pyroxene, and magnetite embedded in an amorphous matrix (Fig. 5). Because the texture and the mineralogy of the particle are quite similar to those of AMMs (*e.g.* KLÖCK *et al.*, 1994), this is most probably an AMM. Most of the olivine grains in this particle do not show terrestrial weathering (Fig. 6).

Magnetite-rich rims can be clearly seen in particle 91-1-C4 (Fig. 7). Because the surface of the particle is uneven, magnetite-rich rims appear around the outline of the particle and around the reentrant holes. The apparent thickness of the magnetite-rich rims is <2 μm. The rims contain coarse-grained (200 nm to >1 μm across) magnetite and olivine, embedded in an amorphous matrix (Fig. 8). Just inside of the rims is composed of fine-grained (<50 nm across) low-Ca pyroxene and rarely olivine, also embedded in an amorphous matrix (Fig. 9).

There are two types of olivine grains with different microstructures in this particle

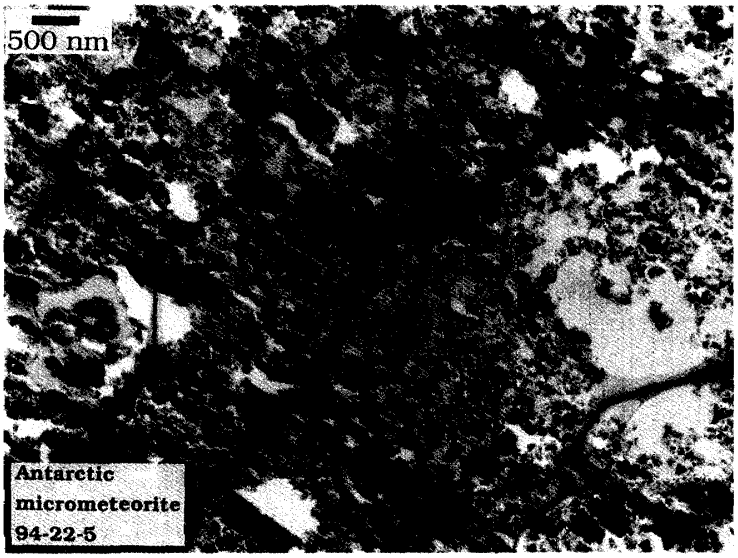

Fig. 4. A low-magnification bright-field TEM image of particle 94-22-5. A microtomed section is embedded in epoxy resin. Grain sizes of the constituent minerals vary from <50 to about 300 nm across. Honeycomb-like network in this figure is a thin supporting plastic film. Lineaments which run from upper left to lower right are artifacts due to slicing.

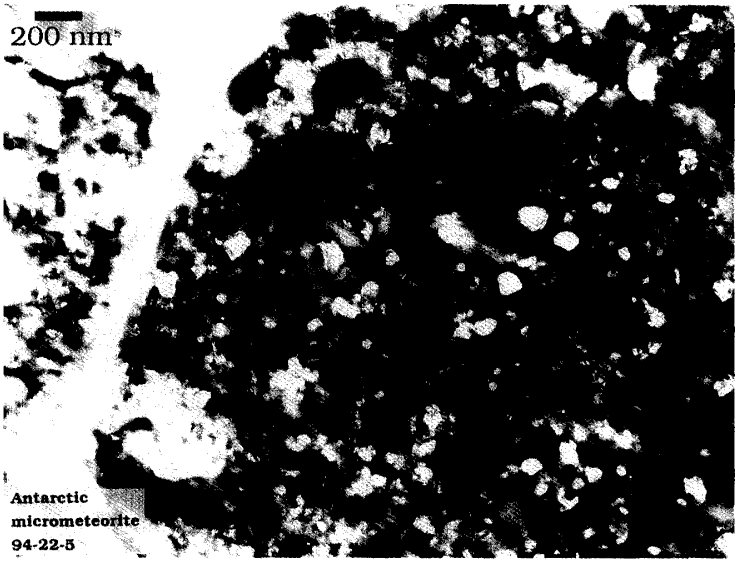

Fig. 5. A dark-field TEM image of a part of the area shown in Fig. 4. This particle consists of fine-grained olivine, low-Ca pyroxene and magnetite embedded in an amorphous matrix. Low-Ca pyroxene crystals show polysynthetic twins. A part of the supporting film is shown in the left corner as a bright band.

Fig. 6. A TEM image of a typical unaltered olivine grain in particle 94-22-5. Olivine crystals are irregular in shape. Parallel bands shown in the upper part of the olivine grain are moire fringes.

Fig. 7. A low-magnification bright-field TEM image of particle 91-1-C4. Magnetite-rich rims are present around the periphery of the particle and around the cavities inside the particle. The dark band shown in the lower right corner is an artifact (a fold of the section). Lineaments shown in this figure are artifacts due to slicing.

(Fig. 10). One is similar to the olivine grains in particle 94-22-5. Another contains lamellar-structured zones. Such olivine crystals viewed perpendicular to the *c*-axis reveal that the lamellar-structured zones are regions of planar channels developed parallel to (001), as shown in Fig. 10. In the selected area electron diffraction patterns of such olivine crystals, diffraction spots show streaks parallel to the *c*-axis. The spacing of the channels are 10–20 nm. Because the length of olivine strips along the *c*-axis is very short, each diffraction spot has streaks along the *c*-axis. Amorphous materials fill these channels.

6.2. Chemical compositions of olivine and low-Ca pyroxene in the AMM candidates

Olivine grains in both of the AMM candidates are Fe-rich (94-22-5: Fo61 to Fo75; 91-1-C4: Fo31 to Fo73). The compositional range of the olivine grains in 91-1-C4 is

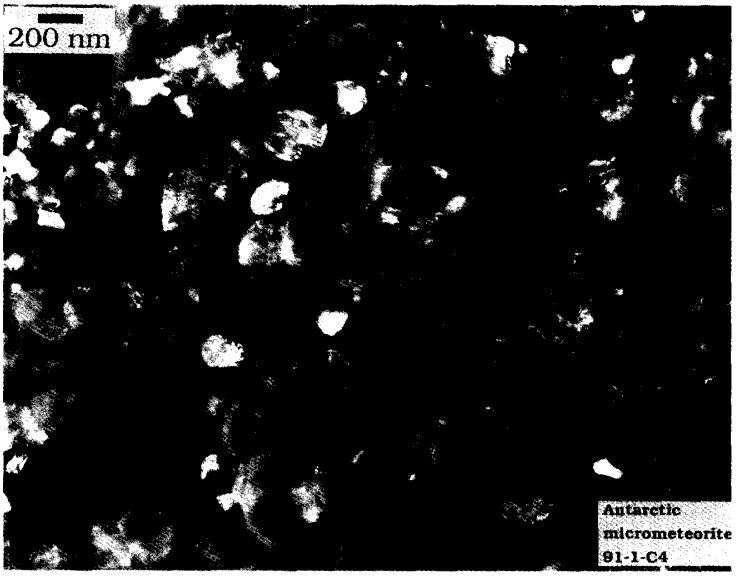

Fig. 8. A dark-field TEM image of a coarse-grained magnetite-rich area in particle 91-1-C4. The area contains magnetite and olivine embedded in an amorphous matrix. A honeycomb-like supporting plastic film is shown as light-gray bands.

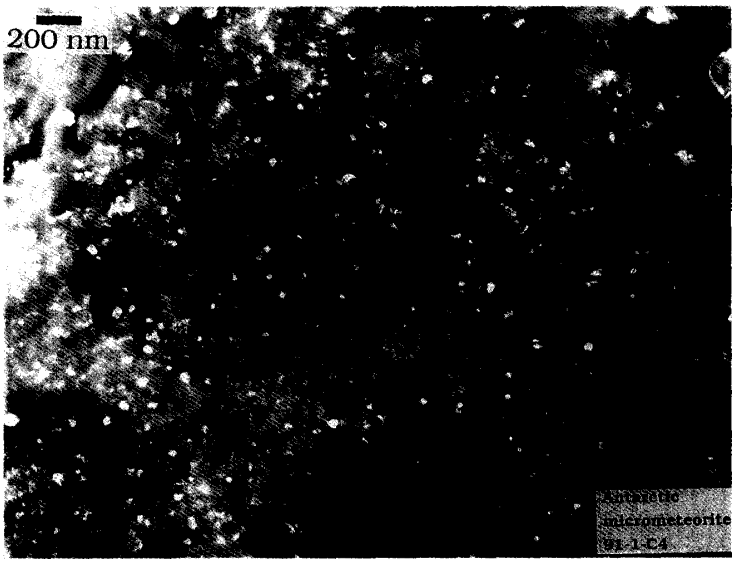

Fig. 9. A dark-field TEM image of a fine-grained area in particle 91-1-C4. This area is composed mainly of low-Ca pyroxene embedded in an amorphous matrix. A honeycomb-like supporting plastic film is shown as vague light-gray bands.

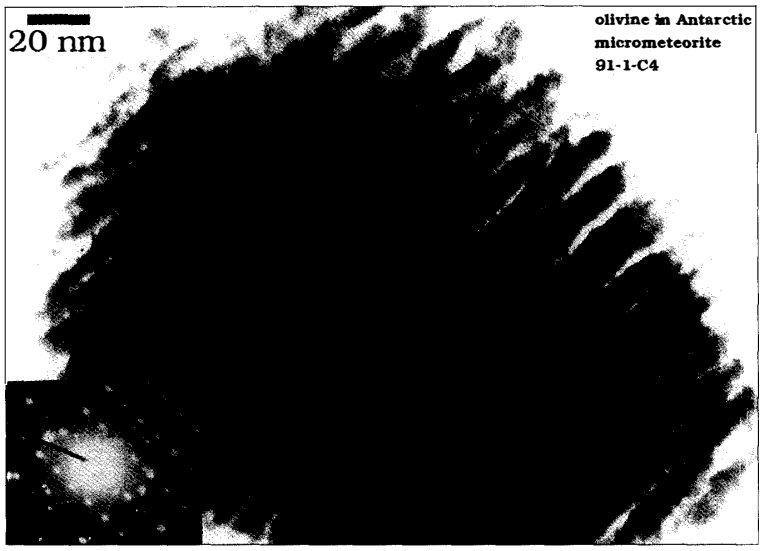

Fig. 10. A TEM image of a typical altered olivine grain in particle 91-1-C4. These olivine grains contain planar channels parallel to (001) plane. Selected area electron diffraction (SAED) pattern shows that diffraction spots have streaks parallel to c of olivine due to the planar channels. Some diffraction spots from the adjacent grains are also shown in the SAED pattern, because the selected area aperture used here could not exclude diffraction from other grains. It is thought that terrestrial weathering proceeded along (001).*

wider than that in 94-22-5. Olivine grains in the two AMM candidates contain relatively high MnO and CaO (Fig. 11 and Table 2) (94-22-5: 0.9–1.6 MnO wt% and 0.5–1.5 wt%; 91-1-C4: 0.4–1.9 MnO wt% and 0–1.1 CaO wt%). The olivine grains in both particles lie significantly above the solar abundance line in a FeO vs MnO diagram (Fig. 11). Particle 91-1-C4 contains two types of olivine grains, as described above. Olivine grains

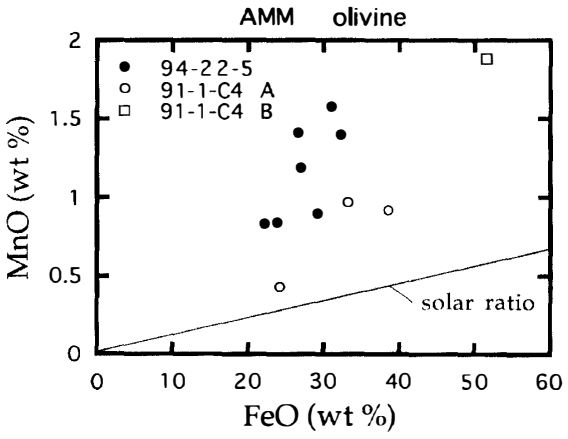

Fig. 11. FeO vs MnO diagram of the newly formed olivine grains in the two AMM candidates. The olivine grains are plotted well above the line with the ratio of solar abundances of iron and manganese. Abbreviations filled circle: unaltered olivine in 94-22-5. open circle (91-1-C4 A): unaltered olivine in 91-1-C4; open square (91-1-C4 B): olivine including planar defects in 91-1-C4.

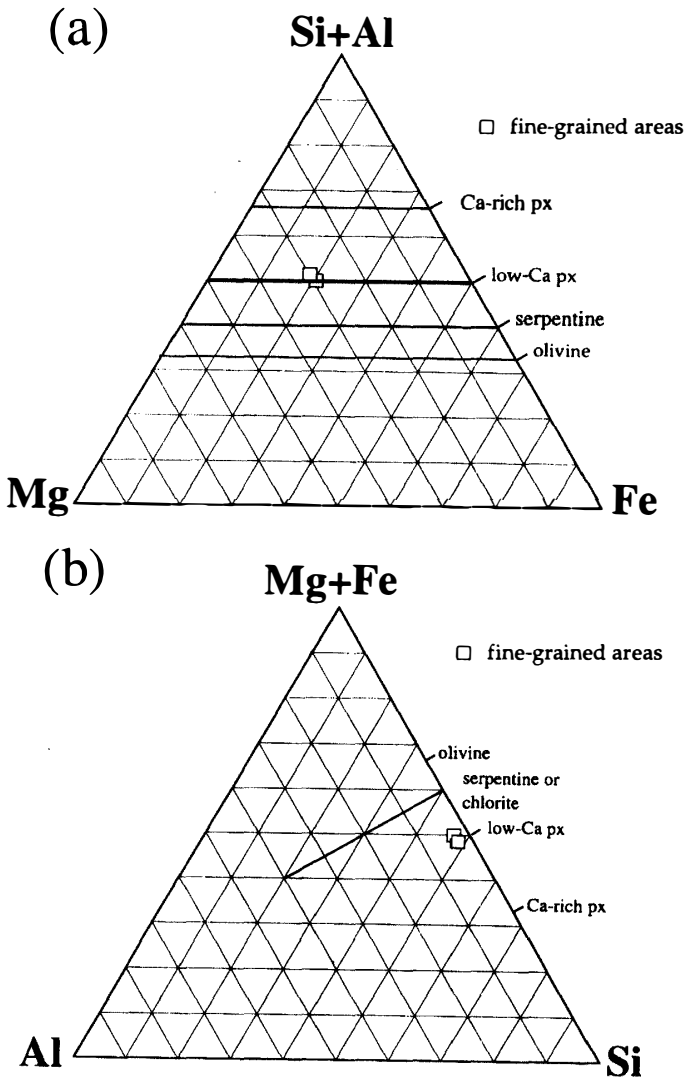

Fig. 12. Atomic (a) (Si+Al)-Mg-Fe and (b) Al-(Mg+Fe)-Si ternary diagrams of the fine-grained areas in particle 91-1C4. Bulk compositions of the fine-grained areas were acquired by broad beam (1 μm in diameter) and lie almost on the low-Ca pyroxene solid solution line. Abbreviations open square: fine-grained area.

similar to those in particle 94-22-5 range from Fo73 to Fo54. On the other hand, olivine grains including planar defects are more Fe-rich, up to Fo31.

Bulk compositions of the fine-grained areas were analyzed by defocused (~1 μm in diameter) beams. Two fine-grained areas were analyzed. They have similar major element abundances (Fig. 12). Their Mg/(Mg+Fe) ratios are 0.59 and 0.62, respectively. They lie almost on the low-Ca pyroxene solid solution line in Fig. 12. Table 2 indicates that the fine-grained areas contain sulfur (shown as SO_3 in Table 2) as well as elements which can be incorporated in low-Ca pyroxene such as Al and Cr. The chemical compositions of the fine-grained areas suggest that the areas analyzed here may contain a small amount of (iron) sulfide or at least some sulfur-bearing phase(s), although sulfides were not identified by TEM observation.

Table 2. Representative compositions of olivine and fine-grained areas in two AMM candidates.

AMM No. minerals	94-22-5 olivine	91-1-C4 olivine	91-1-C4 olivine	91-1-C4 fine-grained area	91-1-C4 fine-grained area
SiO_2	37.15	36.28	32.20	48.77	50.93
TiO_2	b.d.	b.d.	b.d.	b.d.	b.d.
Al_2O_3	b.d.	b.d.	b.d.	2.62	2.61
Cr_2O_3	b.d.	b.d.	b.d.	0.79	0.65
FeO	27.05	33.29	51.62	25.42	23.41
NiO	b.d.	b.d.	b.d.	b.d.	b.d.
MnO	1.19	0.97	1.89	b.d.	b.d.
MgO	33.48	29.03	13.18	20.42	21.05
CaO	1.13	0.43	1.11	b.d.	b.d.
Na_2O	b.d.	b.d.	b.d.	b.d.	b.d.
K_2O	b.d.	b.d.	b.d.	b.d.	b.d.
P_2O_5	b.d.	b.d.	b.d.	b.d.	b.d.
SO_3	b.d.	b.d.	b.d.	1.98	1.34
total wt%	100.00	100.00	100.00	100.00	100.00

All compositions were measured by AEM and normalized to 100 wt%.
Beam diameters: 50–100 nm for olivine grains, 1 μm for fine-grained areas.
b.d.: below detection limits.

7. Discussion

7.1. Other techniques for AMM selection

So, what is the "smoking gun" of extraterrestrial origin for unmelted microparticles in Antarctic ice? The mineralogy, including detection of fission track by solar wind impacts, is surely a strong tool for it but this technique requires considerable difficulties. Detection of isotopic anomaly of heavy elements such as Ir by INAA technique is another choice while estimating cosmic-ray exposure duration with AMS and others requires much larger bulk mass than a 50–100 μm porous particle. Thus we are currently cross checking the potential AMMs between TEM and INAA analyses. Also we are studying one sample of scoriaceous AMMs from the 1992 collection (YANO, 1995) by TEM to understand what level of clarity of mineralogy is available in the "real" AMMs. Unless we succeed in linking their results with the initial survey of morphology and EDS spectrum, it won't be trivial to establish a practical and reliable routine for cataloguing AMMs when the JARE brings tens of thousands of grains back from Antarctic ice in 1999.

We should also investigate the same size range of Maurette's samples from other collection sites in 1994 with an improved "micrometeorite facility" and see if contamination levels and difficulty of AMM detection are reduced. The 1994 collection was the best one made so far, in particular because the blue ice fields were shielded from man made contamination by the heaviest snow falls ever recorded since the building of the French station of Dumont d'Urville, 44 years ago.

7.2. Problems on sample collection and processing

What is more, the samples collected in the expedition at Cap-Prudhomme on 10 January 1994 by Maurette's group witnessed considerably reduced contamination than the 1991 collection faced, because the tubing was replaced by stainless steel of a type used in nuclear reactors. The same careful planning is strongly recommended for the instrumentation of the forthcoming JARE collection.

The sample holders for LV-SEM observation and EDS analysis used in this study are made of brass (an alloy of Cu and Zn). The brass sample holders were used because peak positions of Cu and Zn do not overlap peak positions of elements which are included in common rock forming minerals, and because brass is easy to process. However, analysis of Cu and Zn contents in AMMs may become erroneous due to contamination of these elements from the holders.

Sample holders made of other materials such as graphite, and boron nitride also have shortcomings. Use of graphite holders precludes for the analysis of C, and C stable isotopic composition is important for determination of their origin(s) (*e.g.* GRAHAM *et al.*, 1996). Cubic BN is so hard that it is difficult to make sample holders. Probably Be sample holders are the most suitable for usual elemental analysis. For an example, Be foil which is glued to a carbon holder is routinely used at NASA. However, we did not use Be sample holders because of their expense and the difficulty to process the holders by ourselves due to its toxicity. AMM researchers should discuss the materials for the sample holders before the curation starts.

In this study, sample selection for TEM observation was only based on LV-SEM/EDS observation and analysis, because the main purpose of TEM observation was to assess our sample selection criteria. In order to investigate the petrology and mineralogy of AMMs which were heated weakly during atmospheric entry, observation of cross sections of AMMs is required. TEM study protocols should be based on results of such SEM observation.

7.3. Comparison of texture and mineralogy of the two AMM candidates with previously identified AMMs

KLÖCK *et al.* (1994) reported that most unmelted micrometeorites were in fact strongly heated during atmospheric entry. Due to this transient heating, the original minerals (including phyllosilicates) were transformed into the aggregates of olivine, pyroxene, magnetite, and amorphous materials. Particle 94-22-5 has a very similar texture to that of the strongly heated AMMs (*cf.* Fig. 24 in KLÖCK *et al.*, 1994). The grain sizes of the constituent minerals are also similar to the same AMMs (<50 nm to several hundred nm across). Olivine, pyroxene, and magnetite are uniformly distributed throughout AMM particles. On the other hand, the constituent minerals are distributed heterogeneously in particle 91-1-C4. Fine-grained crystalline areas just inside the magnetite-rich rims are composed mainly of minute (<50 nm across) low-Ca pyroxene crystals.

The grain size variation of the ferromagnesian silicates newly formed due to flash heating was investigated by KLÖCK *et al.* (1994) and GRESHAKE *et al.* (1994). Most of the newly formed ferromagnesian silicates in particle 94-22-5 have grain sizes around 100 nm. Based on the data by GRESHAKE *et al.* (1994), it is estimated that this particle was

heated to about 1100 °C for 20 s. In particle 91-1-C4, grain sizes of the newly formed ferromagnesian silicates is <50 nm except for those of olivine in magnetite rims (about 200 nm). The estimated heating temperature and time duration for the fine-grained areas are 900 °C and 20 s, respectively, according to the data by GRESHAKE *et al.* (1994). An evidence of lower heating temperature for particle 91-1-C4 comes from the presence of sulfur in the fine-grained areas. GRESHAKE *et al.* (1994) reported that 30% of sulfur had been lost during 20 second-heating at 700 °C and that 99% lost during 40 second-heating at 1200 °C. At 900 °C, S may still remain in particle 91-1-C4. Based on the grain sizes of olivine in the magnetite-rich rims, 1200 °C for 20 s was estimated. Higher estimated temperature for the surface of the particle may be explained by processes that might have occurred during atmospheric heating or unequilibrium flash heating. When the particle entered the atmosphere, it would be severely heated and surface volatilization would occur. Due to the latent heat, the temperature inside a particle of this size would never reach that of the surface, if the duration of flash heating was too short. However, in the case of particle 94-22-5, the temperature inside it would approach to the surface temperature due to longer duration of flash heating.

Olivine crystals which were formed during atmospheric entry in the unmelted AMMs are Fo30 to Fo80 (KLÖCK *et al.*, 1994); the AMM candidates are within this range. As already described, there are more ferroan olivine grains in particle 91-1-C4 than in particle 94-22-5. GRESHAKE *et al.* (1994) reported that the olivine newly formed at lower temperature is more ferroan than that formed at higher temperature. Because particle 91-1-C4 contains more ferroan olivine than particle 94-2-5, the data also support the idea that the former was heated to a lower temperature than the latter. The MnO concentration of olivine in chondritic meteorites rarely exceeds 0.5 wt% (KLÖCK *et al.*, 1989), while many olivine grains in IDPs contain >0.5 MnO wt% (KLÖCK *et al.*, 1989). Olivine grains which were formed during atmospheric entry in the AMM candidates contain >0.4 MnO wt% (most are >0.8). These high MnO concentrations may reflect the compositions of the precursor mineral(s) if the mineral(s) would include low-iron and manganese-enriched (LIME) olivine. Olivine grains which were formed during atmospheric entry with considerable amounts of Ni was also reported for the unmelted AMMs (KLÖCK *et al.*, 1994). However, such olivine crystals were not observed in this study.

If 91-1-C4 was originally a hydrous micrometeorite, the bulk compositions of the fine-grained areas would have smectite-like compositions, because most hydrated IDPs include smectite rather than serpentine (*e.g.* ZOLENSKY and LINDSTROM, 1992). Hydrated micrometeorites recovered from Antarctica also contain abundant smectite (*e.g.* KLÖCK *et al.*, 1994). As expected from the fact that the fine-grained areas are composed mainly of low-Ca pyroxene crystals, these areas have low-Ca pyroxene-like compositions. If the precursor was a smectite-rich AMM, there should be abundant Si-rich material to keep the bulk composition smectite-like. The amount of Si-rich material seems to be too deficient to compensate the amounts of the newly formed ferromagnesian silicates and magnetite. On the contrary, the newly formed low-Ca pyroxene crystals do not contain detectable amounts of MnO. The data seem to be consistent with the hydrated precursor hypothesis, because smectite in IDPs (and probably AMMs) does not contain a detectable amount of Mn (*e.g.* BLAKE *et al.*, 1988). If 91-1-C4 was a ferroan serpentine-rich

AMM, magnetite-rich rims may be a complementary part of fine-grained areas. During flash heating, Si may have been fractionated from the surface (magnetite-rich rims) and added to the inner part (fine-grained areas) of 91-1-C4. Although there is no direct evidence for the precursor mineralogy, the available information suggests that this AMM candidate was originally hydrated.

7.4. Evidence for terrestrial weathering of AMMs

In 91-1-C4, ferroan olivine grains (about Fo30) include planar defects parallel to (001) plane. TEM mineralogy of olivine phenocrysts in weathered basalt was studied by EGGERTON (1984) and SMITH *et al.* (1987). These studies revealed that lamellar iddingsite, which was formed in the initial stage of weathering, has planar etch channels parallel to (001). Such planar defects parallel to (001) are formed under acidic aqueous conditions (ISHII *et al.*, in press). The morphology of the planar iddingsite quite resembles the defects that were observed in the ferroan olivine in particle 91-1-C4. Therefore, these data probably display that AMMs (or at least, this AMM candidate) experienced terrestrial weathering, as is the case for the Antarctic meteorites.

It has been reported that terrestrial weathering affected the chemistry of both partially melted and scoriaceous AMMs (*e.g.* FLYNN *et al.*, 1993,1995; KURAT *et al.*, 1994). These data show that AMMs are depleted in Na, Ca, Ni, S, Se, and Zn or enriched in Pb, K, Rb, U, As, and Sb, compared to CI chondrites. FLYNN *et al.* (1995) suggested that the depletions of the elements mentioned above result from weathering. For an example, Fe-Ni sulfides weathered to sulfates and dissolved in water. The large Pb enrichment most likely resulted primarily from terrestrial contamination. In addition to the Fe-Ni sulfide, our data indicate that even olivine crystals suffer from terrestrial weathering if they are ferroan (about Fo30 or less), in the Antarctic environment. RIETMEIJER (1985) pointed out that cryogenic alteration can occur at temperatures below the melting point of water-ice due to the reaction in an interfacial water layer between solid grains and water-ice. In the permanently frozen soils of Antarctica, diagenetic mineral formation occurs on a time scale of 10^4– 10^6 yr (RIETMEIJER, 1985; ZOLENSKY and PACES, 1986). Because the grain size of altering olivine is <50 nm across in 91-1-C4, the formation of iddingsite from ferroan olivine might occur much faster than 10^4 – 10^6 yr.

8. Conclusions and Recommendations

We selected AMM candidates from the unsorted sample set collected by Maurette's group in 1991, based on our initial visual selection (IVS) criteria. After the selection of samples under a stereo-microscope, these samples were observed and analyzed by LV-SEM equipped with EDS. Final selection of AMM candidates was made from LV-SEM/EDS data. Some selected AMM candidates were observed and analyzed by AEM. One AMM candidate, 91-1-C4, contains ferroan (around Fo30) olivine grains which show planar channels parallel to (001). Their textures quite resemble those shown in the initial stage of iddingsite formation of olivine phenocrysts in weathered basalts. This report supports previous contentions that some olivine crystals in AMMs can be altered even in the Antarctic environment. This is important to be noted for the studies of both

mineralogy and chemistry of AMMs.

Our original IVS criteria to choose unmelted AMMs appeared to work, and now we can extend this program to the JARE-39 and 41 AMM collections. However, the ratio of extraterrestrial grains to background terrestrial and artificial grains vary at each collection site and sampling device. Thus, when we receive unsorted JARE-39 samples, we should check the validity of this IVS criteria for the particular sample set by random sampling of, say, ~5% of the total number and analysis by SEM/EDS results. This preliminary assessment is critical to determine the best strategy for curation and cataloguing each collection, and to best facilitate their more detailed studies. In the JARE-39 and -41 campaign, it is also important to collect as small AMMs as stratospheric IDPs for mineralogically unaltered samples. Comparative studies at same sizes will be crucial for understanding of origins of both AMMs and IDPs.

Acknowledgments

We greatly appreciate M. MAURETTE for providing the samples that we represented here. Also M. NAKAMURA and his colleagues at the Tokyo Institute of Technology have kindly allowed us to use their LV-SEM/EDS. The authors are grateful to three referees of G. KURAT, T. NAKAMURA, and M. E. ZOLENSKY for their useful comments that have improved the quality of this paper significantly. HY is supported by the Scientific Research Grant-in-Aid of the Ministry of Education, Science, Culture and Sports of Japan as a part of his research fellowship from the Japanese Society of Promotion of Science. TN is also supported by the Scientific Research Grant-in-Aid of the Ministry of Education, Science, Culture and Sports of Japan (No. 08640600).

References

BLAKE, D.F., MARDINLY, A.J., ECHER, C.J. and BUNCH, T.E. (1988): Analytical electron microscopy of a hydrated interplanetary dust particle. Proc. Lunar Planet. Sci. Conf., 18th, 615–622.

COSMIC DUST PRELIMINARY EXAMINATION TEAM (CDPET) (WARREN, J.L., BARRETT, R.A., DODSON, A.L., WATTS, L.A. and ZOLENSKY, M.E.) (1981–1994): Cosmic Dust Catalog. Houston, NASA/JSC, **1–14** .

EGGERTON, R.A. (1984): Formation of iddingsite rims on olivine: a transmission electron microscope study. Clays Clay Miner., **32**, 1–11.

FLYNN, G.J., SUTTON, S.R. and KLÖCK, W. (1993): Compositions and mineralogies of unmelted polar micrometeorites: Similarities and differences with IDPs and meteorites. Proc. NIPR Symp. Antarct. Meteorites, **6**, 304-324.

FLYNN, G.J., BAJT, S., SUTTON, S.R. and KLÖCK, W. (1995): Chemical composition of large stratospheric dust particles: comparison with stratospheric IDPs, cluster fragments and polar micrometeorites. Lunar and Planetary Science XXVI. Houston, Lunar Planet. Inst., 407–408.

GRAHAM, G.A., WRIGHT, I.P., GRADY, M.M., PERREAU, M., MAURETTE, M. and PILLINGER, C.T. (1996): The C stable isotope composition of Antarctic micrometeorites. Meteorit. Planet. Sci., **31**, Suppl., A53-54.

GRESHAKE, A., KLÖCK, W., ARNDT, P., MAETZ, M. and BISCHOFF, A. (1994): Pulse-heating of fragments from Orgueil (CI): Simulation of atmospheric entry heating of micrometeorites. The Cosmic Dust Connection, ed. by J.M. GREENBERG. Dordrecht, Kluwer Academic Publ., 303–311.

GRÜN, E., ZOOK, H.A., FECHTIG, H. and GIESE, R.H. (1985): Collisional balance of the meteoritic complex. Icarus, **62**, 244–272.

HIGASHI, A., FUJII, Y., TAKAMATSU, S. and WATANABE, R. (1990): SEM observation of microparticles in Antarc-

tic ice cores. Bull. Glacier Res., **8**, 31-53.

HIGASHI, A., SASAKI, K., YANO, H. and OHARA, M. (1992): Regional comparative studies on microparticles in polar ice cores. Proc. NIPR Symp. Polar Meteorol. Glaciol., **6**, 155.

HIGASHI, A. and FUJII, Y. (1994): Studies on microparticles contained in medium-depth ice cores retrieved from east Dronning Maud Land, Antarctica. Ann. Glaciol., **20**, 73–79.

ISHII, K., TORIGOE, K. and HAN, X. (in press): Planar defects in iron-rich olivines produced experimentally in aqueous oxidizing environment. Phys. Chem. Minerals.

KLÖCK, W., THOMAS, K.L., MCKAY, D.S. and PALME, H. (1989): Unusual olivine and pyroxene composition in interplanetary dust and unequilibrated ordinary chondrites. Nature, **339**, 126–128.

KLÖCK, W. and STADERMANN, F.J. (1994): Mineralogical and chemical relationships of interplanetary dust particles, micrometeorites and meteorites. Analysis of Interplanetary Dust, ed. by M.E. ZOLENSKY *et al.* New York, Am. Inst. Phys., 51–87.

KOJIMA, H. (1997): Collection and curation of cosmic dust. Abstract of Jpn Earth and Planet. Sci. Joint. Meeting, March 25–28, Nagoya Univ., 552 (in Japanese).

KUMAI, M. and LANGWAY, C. C., Jr. (1990): Elemental composition, morphology and concentration of particles in firn and ice cores from DYE-3, Greenland. Bull. Glacier Res., **1**, 1–18.

KURAT, G., KOEBERL, C., PRESPER, T., BRANDSTÄTTER, F. and MAURETTE, M. (1994): Petrology and geochemistry of Antarctic micrometeorites. Geochim. Cosmochim. Acta, **58**, 3879–3904.

LOVE, S.G. and BROWNLEE, D.E. (1993): A direct measurement of the terrestrial mass accretion rate of cosmic dust. Science, **262**, 550–553.

MAURETTE, M., OLINGER, C., CHRISTOPHE Michel-Levy, M., KURAT, G., POURCHET, M., BRANDSTÄTTER, F. and BOUROT-DENISE, M. (1991): A collection of diverse micrometeorites retrieved from 100 tons of Antarctic blue ice. Nature, **351**, 44–46.

MAURETTE, M., KURAT, G., PERREAU, M. and ENGRAND, C. (1993): Microanalyses of Cap-Prudhomme Antarctic micrometeorites. Microbeam Analysis, **2**, 239–251.

MAURETTE, M., IMMEL, G., HAMMER, C., HARVEY, R., KURAT, G. and TAYLOR, S. (1994): Collection of IDPs from the Greenland and Antarctic ice sheets. Analysis of Interplanetary Dust, ed. by M.E. ZOLENSKY *et al.* New York, Am. Inst. Phys., 277–289.

NISHIO, F., KATSUSHIMA, T. and OHMAE, H. (1985): Volcanic ash layers in bare ice areas near the Yamato Mountains, Dronning Maud Land and the Allan Hills, Victoria Land, Antarctica. Ann. Glaciol., **1**, 34–41.

RIETMEIJER, F.J.M. (1985): A model for diagenesis in proto-planetary bodies. Nature, **313**, 293–294.

SASE, T., HOSONO, M., UTSUGAWA, T. and AOKI, K. (1988): Opal phytholith analysis of present and buried volcanic ash soils at Te Ngae Road tephra section, Rotorua Basin, North Island, New Zealand–Soil-vegetation relationship for last 20000 years. Quat. Res., **27**, 153–163.

SMITH, K.L., MILNES, A.R. and EGGERTON, R.A. (1987): Weathering of basalt: Formation of iddingsite. Clays Clay Miner., **35**, 418–428.

YADA, T., YANO, H., NAKAMURA, T. and TAKAOKA, N. (1997): Comparisons of unmelted Antarctic micrometeorites with CM chondrites in petrology and mineralogy. Meteorit. Planet. Sci., **32**, A144.

YANO, H. (1991): Identification of Solid Microparticles in Ice Cores and Surface Snow from Asuka Station, Antarctica -Comparative Studies with NASA Cosmic Dust Catalog and Microparticles Retrieved at Mizuho Station and Advance Camp, Antarctica-. B. Sc. Thesis, International Christian University, Tokyo.

YANO, H. (1995): The Physics and Chemistry of Hypervelocity Impact Signatures on Spacecraft: Meteoroids and Space Debris. Ph.D. Thesis, University of Kent at Canterbury, Kent, U. K.

YANO, H., ENGLAND, C. and MAURETTE, M. (1996): Hypervelocity impact experiments using Antarctic micrometeorites. Antarctic Meteorites XXI. Tokyo, Natl Inst. Polar Res., 213–215.

ZOLENSKY, M.E. and LINDSTROM, D.J. (1992): Mineralogy of 12 large "chondritic" interplanetary dust particles. Lunar Planet. Sci. Conf., 19th, 161–169.

ZOLENSKY, M.E. and PACES, J. (1986): Alteration of tephra in glacial ice by "unfrozen water". GSA Abstracts with Programs, **18**, 801.

ZOLENSKY, M.E., BARRETT, R.A., HRUBESH, L., HÖRZ, F. and LINDSTROM, D. (1990): Cosmic dust capture simulation experiments using silica aerogels. Lunar and Planetary Science XXI. Houston, Lunar Planet.

Inst., 1381–1382.
ZOLENSKY, M.E., ZOOK, H.A., HÖRZ, F., ATOKINSON, D.R., COOBS, C.R., WATTS, A.J., DARDANO, C.B., SEE, T.H., SIMON, C.G. and KINARD, W.H. (1993): Interim report of the meteoroid and debris special investigation group. Proc. Second LDEF Post-Retrieval Symp., NASA CP-3194, 277-302.
ZOLENSKY, M.E., WILSON, T.L., RIETMEIJER, F.J.M. and FLYNN, G.J. (1974): Analysis of Interplanetary Dust. New York, Am. Inst. Phys., 357 p.

(Received September 16, 1997; Revised manuscript accepted January 21, 1998)